

LA-5498-MS

INFORMAL REPORT

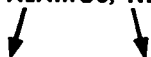
63

Analysis of Pellet-to-Pellet Data from Nuclear Reactor Fuel Rod Scanning Systems

L



los alamos
scientific laboratory
of the University of California
LOS ALAMOS, NEW MEXICO 87544



UNITED STATES
ATOMIC ENERGY COMMISSION
CONTRACT W-7405-ENG. 36

This report was prepared as an account of work sponsored by the United States Government. Neither the United States nor the United States Atomic Energy Commission, nor any of their employees, nor any of their contractors, subcontractors, or their employees, makes any warranty, express or implied, or assumes any legal liability or responsibility for the accuracy, completeness or usefulness of any information, apparatus, product or process disclosed, or represents that its use would not infringe privately owned rights.

In the interest of prompt distribution, this LAMS report was not edited by the Technical Information staff.

Printed in the United States of America. Available from
National Technical Information Service
U. S. Department of Commerce
5285 Port Royal Road
Springfield, Virginia 22151
Price: Printed Copy \$4.00; Microfiche \$1.45

LA-5498-MS

Informal Report

UC-15

ISSUED: January 1974



Analysis of Pellet-to-Pellet Data from Nuclear Reactor Fuel Rod Scanning Systems

by

R. A. Forster



TABLE OF CONTENTS

I. INTRODUCTION	1
II. THEORY OF CALCULATING THE MEASURED RESPONSE	2
A. Detector Response Function	2
B. Equations	3
III. PELLETT POSITIONS RELATIVE TO THE DETECTOR AND Δt	5
IV. MODELS	5
A. One-Point Models	6
B. Two-Point Models	9
V. NUMERICAL RESULTS	10
A. One-Point Models	10
B. Two-Point Models	15
VI. CONCLUSIONS	15
Appendix: THE ONE-POINT MODEL FOR THE WORST MEASURING POSITION FOR TWO AND THREE DETECTORS	17

DEFINITION OF SYMBOLS

- a = full width at half-maximum (FWHM) of detector response function
 A = area between $\mu - z$ and $\mu + z$ of the normal distribution
 A_γ = area between $\mu - \gamma\sigma$ and $\mu + \gamma\sigma$ of the normal distribution
 A_δ = area between $\mu - \delta\sigma$ and $\mu + \delta\sigma$ of the normal distribution
 $b = \sqrt{\ln 2}/a$ [see Eq. (1)]
 \dot{B} = effective emission rate (i. e., the observed count rate in a detector) of a bad pellet
 \dot{B}_H = minimum detectable high off-specs pellet effective emission rate
 \dot{B}_L = minimum detectable low off-specs pellet effective emission rate
 \dot{B}_j = effective emission rate of the j^{th} pellet in a fuel rod [see Eq. (6)]
 F = length of good fuel on each side of a bad pellet [see Eq. (7)]
 L = length of the bad pellet
 L_j = length of the j^{th} pellet in a fuel rod [see Eq. (6)]
 n = number of detectors measuring the delayed gamma rays from the fuel rod
 N = number of pellets in a fuel rod [see Eq. (6)]
 $R(y)$ = detector response function [see Eq. (1)]
 \dot{S} = observed count rate in the detector from a rod of good or in-specs pellets
 \dot{S}_H = minimum detectable high observed count rate (see Figs. 6, 7, and 8)
 \dot{S}_L = minimum detectable low observed count rate (see Figs. 6, 7, and 8)
 $\dot{S}\Delta t$ = expected value of the TOC in a time interval Δt
 TOC = total observed counts from one detector in a time Δt
 x = position of the trailing edge of a bad pellet surrounded by good pellets [see Eqs. (3), (5), (7), and (8)]
 x_1 = position of the trailing edge of the bad pellet at the beginning of the Δt time interval [see Eqs. (5), (7), and (8)]
 x_2 = position of the trailing edge of the bad pellet at the end of the Δt time interval [see Eqs. (5), (7), and (8)]
 x_j = position of the trailing edge of the j^{th} pellet [see Eq. (6)]
 $x_{1,j}$ = position of the trailing edge of the j^{th} pellet at the beginning of time interval Δt [see Eq. (6)]
 $x_{2,j}$ = position of the trailing edge of the j^{th} pellet at the end of time interval Δt [see Eq. (6)]
 \dot{X} = rate at which a fuel rod is pushed through the scanning system
 y = dummy variable signifying position in detector response function
 γ = tolerance interval of $\pm \gamma\sqrt{\dot{S}\Delta t}$ about $\dot{S}\Delta t$ defining region of acceptance (see Fig. 8)
 δ = distance below $\dot{S}_H\Delta t$ (or above $\dot{S}_L\Delta t$) to the tolerance interval around $\dot{S}\Delta t$
 δ_w = distance below $\dot{S}_H\Delta t$ (or above $\dot{S}_L\Delta t$) to the tolerance interval around $\dot{S}\Delta t$ for two measurements in the worst position
 Δt = **time** interval during which detector counts are integrated
 σ = standard deviation
 μ = (mean) parameter of a Poisson distribution

ANALYSIS OF PELLETT-TO-PELLET DATA FROM
NUCLEAR REACTOR FUEL ROD SCANNING SYSTEMS

by

R. A. Forster

ABSTRACT

The problem of analyzing a sequence of measured points from a nuclear reactor fuel rod scanning system to detect a pellet outside of specifications is examined in detail. A theory of calculating the expected values of the measured points is presented which can be applied to any system with continuous scanning. Simple models are developed to accept or reject a fuel rod on the basis of the sequence of measured points. As an example, numerical results for optimizing various operating parameters and determining the sensitivity of a light water reactor fuel pellet-to-pellet system using the theory and the models are discussed.

I. INTRODUCTION

Nuclear reactor fuel rods are composed of an integer number of fuel pellets containing fissile material (^{233}U , ^{235}U , and/or ^{239}Pu). The length of each pellet is typically between one and two times its diameter, depending on the manufacturer and reactor type; thus, each fuel rod contains on the order of 100-200 pellets for both fast and thermal reactors. The axial profile of the fissile loading for each rod in a given reactor is specified by the reactor vendor.

Several quality control problems concerning the pellets arise in the manufacture of fuel rods. For example, a rod could contain pellets of a uniform, but different, enrichment than is required. This problem can be detected by using a fuel rod assay system to measure the total fissile content of the rod. A much more difficult situation to detect is a rod which contains the required

nominal enrichment(s) except for one or more anomalous pellets.

Until recently, rapid pellet-to-pellet scanning equipment for fuel rods was not available. At the present time, LASL's Nuclear Analysis Research Group has installed such a system for fast reactor fuel at Westinghouse--Hanford Engineering Development Laboratory (HEDL) and constructed a prototype system for light water reactor (LWR) fuel. Both systems detect gamma rays emitted from the fissile component of the fuel as the basis for pellet-to-pellet examination.

Pellet-to-pellet data can be analyzed in two basic ways: (1) using a rate meter to yield a continuous profile, and (2) integrating the observed counts over a time interval Δt , thereby producing a sequence of total observed count (TOC) points describing the axial fissile profile of the rod. This report will focus on the second

technique. Several methods are available to treat a sequence of numbers, e. g., data smoothing and the fast Fourier transform technique. The purpose of this report is to discuss simple models by which a rod is accepted [contains pellets of the required nominal enrichment(s)] or is rejected [all pellets are not of the required nominal enrichment(s)] on the basis of the sequence of data points. The scanning procedure is assumed to be continuous or stepwise with the length of the step being much less than the length of a pellet.

LASL's Pin and Pellet Assay System (PAPAS)¹ for LWR fuel will be used as the basis for discussion of the models. The operating characteristics of the system will be examined as a function of several variables, using the models. Minimum detectable out-of-specifications (off-specs) pellets will be examined using the models for one or more measurements of the rod.

II. THEORY OF CALCULATING THE MEASURED RESPONSE

A mathematical model of a pellet-to-pellet scanning system is required to calculate the expected value of the measured response and to determine the sensitivity of the scan to variations in the fissile material profile. Three characteristics of the scanning system are required to predict the expected value of the measured response: (1) the detector response $R(y)$ as a function of position y in the detector, (2) the observed count rate in the detector of \dot{S} counts/sec from a rod containing good pellets, and (3) the relative rate of motion between the rod and the detector.

A. Detector Response Function

The detector response function $R(y)$ can be characterized by the full width at half-maximum (FWHM) of the detector and $\int_{-\infty}^{\infty} R(y)dy$. The detector used in PAPAS (see Fig. 1) for the pellet-to-pellet measurement is a 2- by 2- by $\frac{3}{4}$ -in. NaI with a rod $\frac{3}{4}$ -in. diam through-hole to count the delayed gamma rays emitted from the thermal neutron induced fissions in the fuel. The gamma-ray counts

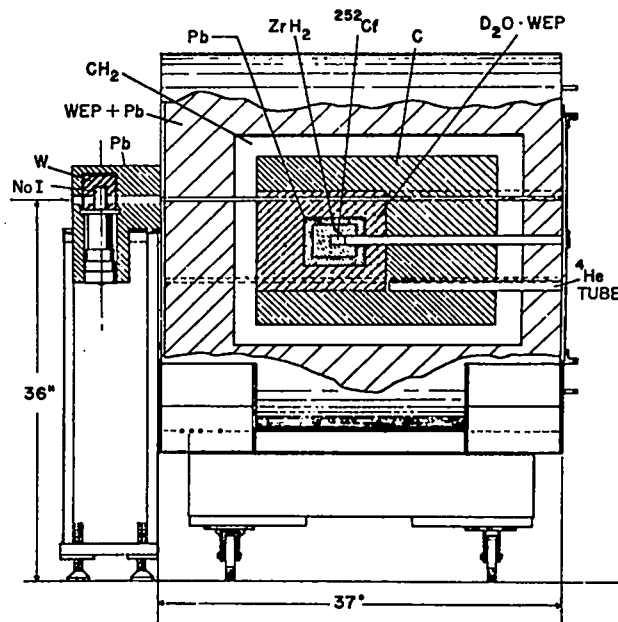


Fig. 1. Thermal neutron ^{252}Cf fuel rod assay system with modifications for pellet-to-pellet scan. The ^4He neutron detectors in the carbon core count the prompt fission neutrons for total fissile determination, and the NaI detectors near the fuel rod exit channel count the delayed gamma rays for pellet-to-pellet determination. Direction of fuel rod travel is from right to left.

are integrated over a time interval of Δt seconds; thus, the output of the scan of a rod is available as a sequence of TOC points as illustrated in Fig. 2.

The response function of the detector, shown in Fig. 3, was measured at several positions using a single PWR fuel pellet. The solid line in Fig. 3 represents the mathematical model (the Gaussian or normal distribution) used to simulate the detector response, which is written as

$$R(y) = \frac{b}{\sqrt{\pi}} e^{-b^2 y^2}, \quad (1)$$

where $b = \sqrt{\ln 2/a}$, $a = \text{FWHM}$ (1.2 in.) and y is the position relative to the center of the detector. Note that $\int_{-\infty}^{\infty} R(y)dy = 1$. Thus, the observed count rate \dot{S} counts/sec is obtained by scaling the integral of $R(y)$ by \dot{S} .

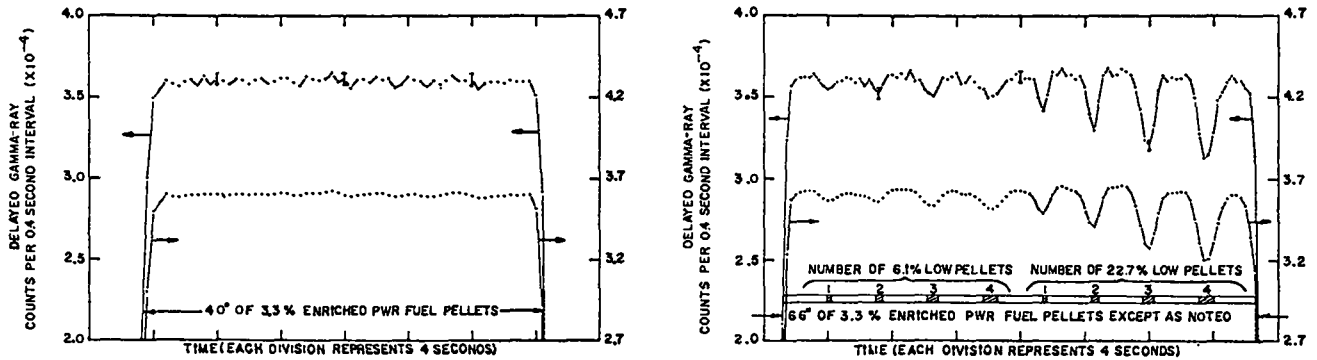


Fig. 2. (Left) A typical delayed gamma-ray scan of a 40-in. -long 3.3% PWR fuel rod. The lower curve is a smoothed version of the raw data in the upper curve (the error bars represent 2σ uncertainties). Each point represents the total counts accumulated in 0.4 sec for a rod feed rate of 8 ft/min. (Right) A typical delayed gamma-ray scan of a 66-in. -long 3.3% PWR fuel rod with pellets of lower enrichments interspersed as shown above. The lower curve is a smoothed version of the raw data in the upper curve (the error bars represent 2σ uncertainties). Each point represents the total counts accumulated in 0.4 sec for a rod feed rate of 8 ft/min.

B. Equations

Several simple examples of reactor fuel rod pellet configurations are considered to develop the equations for the TOC. The equations are written for a general $R(y)$ as well as the specific case given in Eq. (1).

1. A Stationary Rod of Uniform Pellets.

For a rod of uniform pellets with an observed count rate in the detector of \dot{S} counts/sec, the TOC in a time interval Δt is

$$\text{TOC} = \dot{S} \int_{\Delta t} \int_{-\infty}^{\infty} R(y) dy dt = \dot{S} \Delta t. \quad (2)$$

The rod is assumed to be much longer than the width of the detector and is therefore effectively infinite in length.

2. A Single Stationary Pellet. The TOC in a time interval Δt from a single pellet of length L whose trailing edge (with respect to the direction of travel) is at position x relative to the center of the detector and yields \dot{B} counts/sec for a rod is

$$\text{TOC} = \dot{B} \int_{\Delta t} \int_x^{x+L} R(y) dy dt = \frac{\dot{B} \Delta t}{2} (\text{ERF}[b(x+L)] - \text{ERF}[bx]) \quad (3)$$

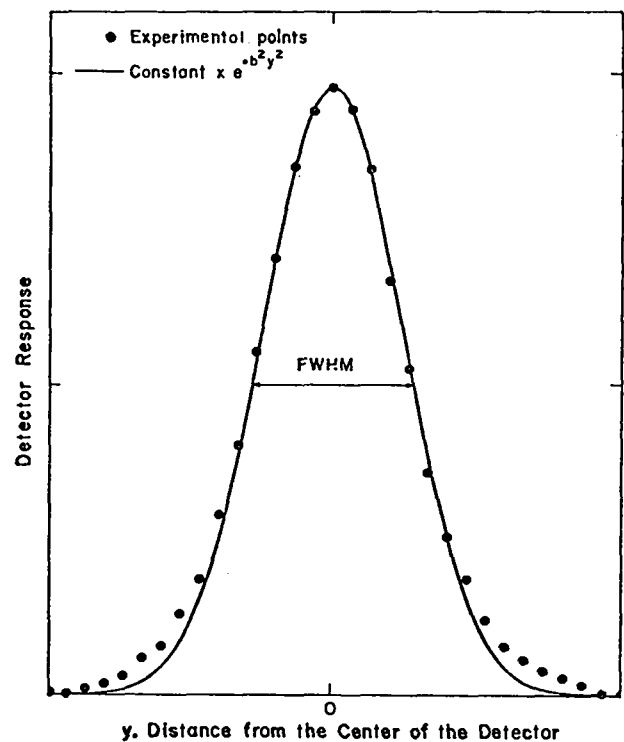


Fig. 3. Response function of the NaI detector at the exit of an irradiation channel in PAPAS.

where ERF(Z) is the error function and is given by

$$\text{ERF}(Z) = \frac{2}{\sqrt{\pi}} \int_0^Z e^{-w^2} dw. \quad (4)$$

3. A Single Moving Pellet. If the pellet is moving, then the position x is a function of time [$x(t) = x_1 + \dot{X}t$ and $dx = \dot{X}dt$] and Eq. (3) becomes, by transforming time t to position x ,

$$\begin{aligned} \text{TOC} &= \frac{\dot{B}}{\dot{X}} \int_{x_1}^{x_2} \int_x^{x+L} R(y) dy dx \\ &= \frac{\dot{B}}{2\dot{X}b} \sum_{i=1}^2 (-1)^i \left\{ b(x_i + L) \text{ERF}[b(x_i + L)] \right. \\ &\quad \left. - bx_i \text{ERF}[bx_i] + \frac{1}{\sqrt{\pi}} \left(e^{-b^2(x_i+L)^2} - e^{-b^2x_i^2} \right) \right\}, \quad (5) \end{aligned}$$

where x_1 and x_2 are the positions of the pellet's trailing edge at the beginning and end of the time interval Δt and \dot{X} is the rate of rod travel ($x_2 = x_1 + \dot{X}\Delta t$).

4. A Moving Rod Composed of Different Pellets. For the general case of a rod composed of N pellets of different lengths and enrichments, the TOC in a time Δt would be

$$\begin{aligned} \text{TOC} &= \frac{1}{\dot{X}} \sum_{j=1}^N \dot{B}_j \int_{x_{1,j}}^{x_{2,j}} \int_{x_j}^{x_j+L_j} R(y) dy dx_j \\ &= \frac{1}{2\dot{X}b} \sum_{j=1}^N \dot{B}_j \sum_{i=1}^2 (-1)^i \left\{ b(x_{i,j} + L_j) \right. \\ &\quad \left. \cdot \text{ERF}[b(x_{i,j} + L_j)] - bx_{i,j} \text{ERF}[bx_{i,j}] \right. \\ &\quad \left. + \frac{1}{\sqrt{\pi}} \left(e^{-b^2(x_{i,j}+L_j)^2} - e^{-b^2x_{i,j}^2} \right) \right\}, \quad (6) \end{aligned}$$

where \dot{B}_j is the observed count rate for a rod of the j^{th} material, L_j is the length of the j^{th} pellet, and $x_{1,j}$ and $x_{2,j}$ are the positions of the j^{th} pellet's trailing edge at the beginning and end of the

time interval Δt . Equation (6) thus allows the expected value of the measured response to be calculated for any conceivable group of pellets that comprise a fuel rod.

5. A Moving Rod Containing One Anomalous Pellet. The TOC in a time interval Δt from a rod composed of a single bad pellet (\dot{B} counts/sec) of arbitrary length L surrounded on both sides by good fuel (\dot{S} counts/sec) of length F can be written from Eq. (6) as

$$\begin{aligned} \text{TOC} &= \frac{1}{\dot{X}} \left[\dot{S} \int_{x_1-F}^{x_2-F} \int_{x-F}^x R(y) dy d(x-F) \right. \\ &\quad \left. + \dot{B} \int_{x_1}^{x_2} \int_x^{x+L} R(y) dy dx \right. \\ &\quad \left. + \dot{S} \int_{x_1+L}^{x_2+L} \int_{x+L}^{x+L+F} (R(y) dy d(x+L)) \right]. \quad (7) \end{aligned}$$

As $F \rightarrow \infty$, Eq. (7) can be written as

$$\begin{aligned} \text{TOC} &= \frac{1}{\dot{X}} \left[\dot{S} \int_{x_1}^{x_2} \int_{-\infty}^x R(y) dy dx + \dot{B} \int_{x_1}^{x_2} \int_x^{x+L} R(y) dy dx \right. \\ &\quad \left. + \dot{S} \int_{x_1}^{x_2} \int_{x+L}^{\infty} R(y) dy dx \right] \\ &= \dot{S}\Delta t + \left(\frac{\dot{B} - \dot{S}}{2\dot{X}b} \right) \sum_{i=1}^2 (-1)^i \left\{ b(x_i + L) \right. \\ &\quad \left. \cdot \text{ERF}[b(x_i + L)] - bx_i \text{ERF}[bx_i] \right. \\ &\quad \left. + \frac{1}{\sqrt{\pi}} \left(e^{-b^2(x_i+L)^2} - e^{-b^2x_i^2} \right) \right\}. \quad (8) \end{aligned}$$

The remainder of this report will consider the problem of detecting a bad pellet (\dot{B} counts/sec) of length L surrounded on both sides by an infinite length (relative to the detector width) of good pellets (\dot{S} counts/sec), i. e., examining numerical solutions of Eq. (8).

III. PELLETS POSITIONS RELATIVE TO THE DETECTOR AND Δt

A pellet will make its largest contribution to a given TOC point when the pellet has crossed the center of the detector during the time interval Δt associated with that point. Figure 4 shows the two extreme pellet measurement positions (labeled "best" and "worst") with respect to the detector response function.

The best possible position for a single bad pellet (surrounded by good pellets) to be detected in a single measurement is for it to be located at the center of the detector halfway through the Δt counting time, as shown in Fig. 4. In the best position, the bad pellet will make its largest possible contribution to the measured response; therefore, the minimum detectable off-specs pellet for this position is the best that the system can do for one measurement of duration Δt seconds.

The worst position for a single measurement of a bad pellet would occur when the pellet

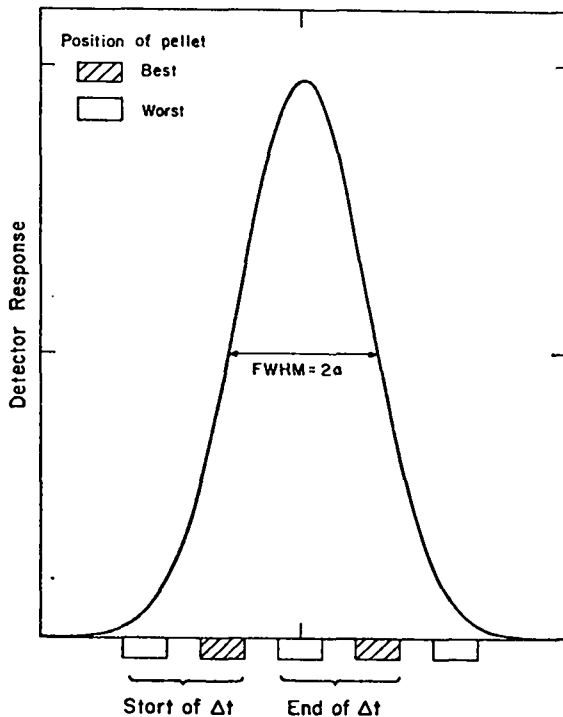


Fig. 4. The two extreme (best and worst) pellet measurement positions with respect to the detector for a counting time of Δt . Direction of travel is from left to right.

is located at the center of the detector at the conclusion (or start) of a Δt counting interval. It is important to note that the worst position for a pellet yields two equivalent measurements of the pellet.

An average position represents the expected pellet position, i. e., halfway between the best and worst positions.

The models discussed in this report assume that the measurement which either precedes or follows a measurement in the best position will most likely not indicate the presence of the bad pellet. This is tantamount to requiring that the pellet in the best position pass completely through the detector during the Δt time interval. This assumption simplifies the analysis since only one measurement in the best position and, at most, two in the worst position need to be considered. As is shown later, this is a valid assumption for the system under consideration. It is also assumed that in the case of multiple detectors each detector is identical and views each pellet in the same position. This is true for a uniform feed rate with each detector starting to count when the fuel reaches a given fixed position relative to the detector.

IV. MODELS

Two simple models will be examined to determine their ability to reject rods with bad pellets. In the first model, denoted the one-point model, a single outlying TOC point is used to classify a rod as a reject. In the second model, labeled the two-point model, two adjacent points are used.

A graph representing the behavior of the observed good count rate \dot{S} (corrected for background) of uniformly enriched PWR fuel sections from PAPAS vs ^{235}U mass in the rod is shown in Fig. 5. The nonlinearity in the curve is caused by the self-shielding of the interrogating thermal neutrons in PAPAS. The minimum detectable off-specs pellet rate \dot{B} of each model and pellet position will be expressed as a percentage of \dot{S} rather

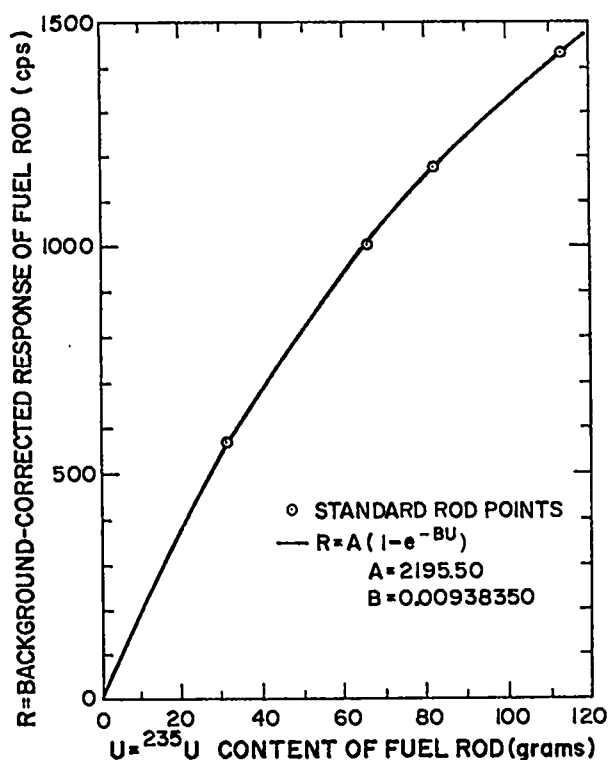


Fig. 5. Response R (proportional to \dot{S}) as a function of the ^{235}U content of PWR fuel with different enrichments.

than an absolute difference from \dot{S} because the former is more useful in the nuclear industry. Figure 5 is needed to transform the minimum detectable count rate differences to minimum detectable pellet enrichment (^{235}U mass) differences.

PAPAS could have one or more detectors at the exit end to measure the rods. The cases of one and multiple detectors will be treated separately. The models considered are based only on "counting statistics". For instruments where the square root of the number of counts ($\sqrt{\text{TOC}}$) in a time interval Δt is not a good estimate of the standard deviation of the TOC, measured estimates should be used. The basic models still apply, and the estimates based on counting statistics represent the lower limit of bad pellet detection for an instrument at the stated level of confidence.

A. One-Point Models

A one-point model is defined as requiring a single point of the sequence of measured points

for one fuel rod to lie outside of a specified tolerance interval about a known nominal mean value of the TOC points for a specified rod fissile loading to cause rejection of the rod. The nominal level is known from standard rod measurements or from averaging the TOC points of a given rod. This model is especially well suited for pellets measured in the best position. The model must reject as few good rods and as many bad rods (i. e., rods containing at least one off-specs pellet) as possible. The model definition of a minimum detectable off-specs pellet is the minimum detectable difference in observed rates between the bad pellet and its neighbors at a specified level of confidence.

1. One Detector. A simple criterion for detecting a bad pellet is the following. Assume that the expected value for a total (corrected for background) number of counts observed in Δt seconds from a rod containing uniform, good pellets is $\dot{S}\Delta t$. The TOC points will be Poisson distributed with mean $\dot{S}\Delta t$ and variance $\dot{S}\Delta t$, assuming that no other random errors are present such as electronic drifts, rod positioning, etc. The one-point, one-detector model is defined so as to interpret any TOC point which lies outside the "tolerance interval" $\dot{S}\Delta t \pm 4\sqrt{\dot{S}\Delta t}$ as a measurement which included a bad pellet, i. e., a pellet unlike its neighbors. The number four multiplying the $\sqrt{\dot{S}\Delta t}$ is an arbitrary choice and can be any value desired consistent with good rod rejection criteria. A single measurement producing a TOC point for good fuel pellets (more than one pellet contributes to a measurement at a time) will statistically lie outside of this tolerance interval for 0.00634% of all measurements; thus, if the sequence of measured points for a rod includes 200 points, 1.27% of the good rods will be rejected: about one rod out of eighty. This seems to be a reasonable rejection criterion, particularly if the rejected rods are remeasured to determine whether the bad point(s) occur at the same axial position along the rod. A second false rejecting point anywhere in the 200-point sequence would cause 0.0161% of the good fuel rods (one rod

in 6220 rods) to be rejected; however, if the second false rejecting point is required to repeat at the same position on the rod, then $4.02 \times 10^{-5}\%$ of the good rods (one rod in 2.49×10^6) will be rejected as faulty. The results of the second measurement could also be added to the first sequence of TOC points, if appropriate, to yield a more precisely (relative) known TOC sequence.

On the other hand, one would like to be quite certain that a bad pellet will be detected. In order to satisfy both good and bad rod rejection criteria, consider the model described in Fig. 6 for a series of TOC points measured by one detector scanning a fuel rod. A bad pellet with an observed rate (for a rod) of $\dot{B}_H > \dot{S}$ (or $\dot{B}_L < \dot{S}$) which will yield the $\dot{S}_H \Delta t$ (or $\dot{S}_L \Delta t$) counts in Fig. 6 will be detected 97.73% of the time for a single measurement because this percentage of the Poisson (assumed normal) distribution is above (or below) the 4σ tolerance interval of $\dot{S} \Delta t$. Once \dot{S} and Δt are known, \dot{S}_H (or \dot{S}_L) can be determined such that the relationship of $\dot{S}_H \Delta t$ (or $\dot{S}_L \Delta t$) to $\dot{S} \Delta t$ in Fig. 6 is satisfied. Since the TOC value is known, \dot{B}_H (or \dot{B}_L) can then be calculated from Eq. (8) as a function of Δt , pellet length, rod feed rate, effective good pellet emission rate \dot{S} , the FWHM of the detector, and the position of the bad pellet as it is being counted. \dot{B}_H (or \dot{B}_L) is defined as the minimum detectable high (or low)

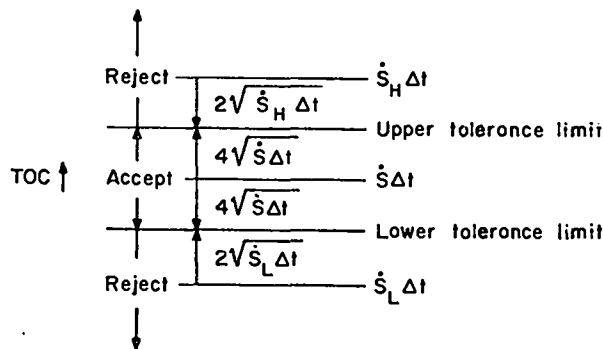


Fig. 6. One-point model for rejecting a rod with one TOC point in the reject region.

observed count rate which will be detected in 97.73% of the measurements for this model. Any pellet that is further out of specs than \dot{B}_H (or \dot{B}_L) will be detected by more than 97.73% of the measurements.

This model can be modified for the worst pellet measurement position by using the fact that there are two identical measurements. Since the expected value of the two points is the same, there are two chances to produce one point outside of the $\dot{S} \Delta t \pm 4\sqrt{\dot{S} \Delta t}$ tolerance interval. The probability of accepting a bad rod with one minimum detectable off-specs pellet in two measurements in the worst position is $\left(\frac{1-A}{2}\right)^2 = (1 - 0.9773)$ where A is the area between $\mu-z$ and $\mu+z$ of the normal distribution (mean $\dot{S}_H \Delta t$ or $\dot{S}_L \Delta t$). Solving for A and finding the appropriate number to replace the 2 (the multiplier of $\sqrt{\dot{S}_H \Delta t}$ and $\sqrt{\dot{S}_L \Delta t}$) in Fig. 6 yields the equivalent model for two measurements in the worst position, which is shown in Fig. 7. Thus, even though one measurement of a bad pellet in the worst position is not as sensitive as a single measurement in the best position, the two measurements combined in the above way approach the best position's minimum detectable pellet, as shown by the numerical results in Sec. V.

2. Multiple Detectors. If two or more detectors (all identical) are located at the exit end of PAPAS, the additional measurements using the same Δt will enable pellets which are less out

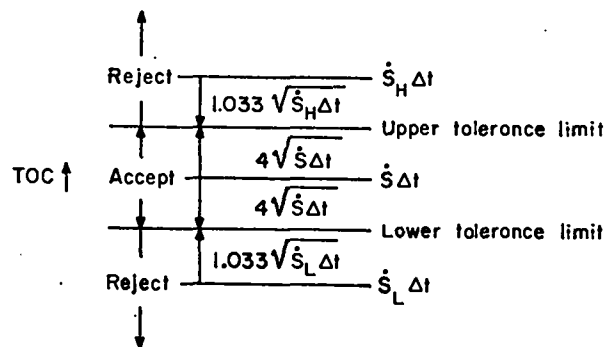


Fig. 7. One-point model for the two equivalent measurements in the worst measuring position.

of specs than in the one-detector model to be unmasked. This model is also most applicable to pellets near the best measuring position because they are measured just once, but quite well, in each detector. It is assumed that the observed rate in all detectors is the same and that there is no cross-talk between detectors.

Consider Fig. 8. In order to reject a rod, at least one point at the same axial rod position from each detector must be outside and to the same side of the tolerance interval. The values of γ and δ must be determined such that the number of good rods rejected and the number of bad rods rejected containing a minimum detectable bad pellet (i. e., producing the expected TOC of $\dot{S}_H \Delta t$ or $\dot{S}_L \Delta t$) are the same as in the one detector model (0.00634% and 97.73%, respectively).

Gamma (γ) can be found in the following way. Define A_γ to be the area of the normal curve (mean of $\dot{S} \Delta t$) between $\gamma\sigma$ and $-\gamma\sigma$. Then the probability that a good rod will be rejected is $(1 - A_\gamma) \left(\frac{1 - A_\gamma}{2}\right)^{n-1}$ where n is the number of detectors. The above expression is set equal to 0.000634 and A_γ is determined. The value of γ which yields the corresponding A_γ can then be found from tables of normal distribution central areas.²

Delta (δ) is determined in a similar manner, except that the expression for the probability

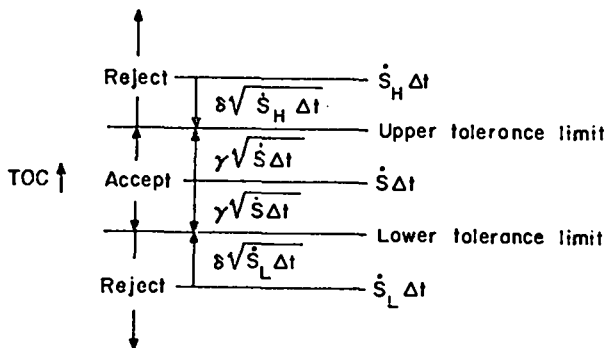


Fig. 8. General model for rejection of a rod which has at least one TOC point in the reject region.

of rejecting a rod with one TOC point of expected value $\dot{S}_H \Delta t$ (or $\dot{S}_L \Delta t$) in a single measurement $[A_\delta + (1 - A_\delta)/2]^n$ is set equal to 0.9773. The results for the δ s and γ s are listed in Table I for up to five detectors. The third column ($\gamma + \delta$) is a measure of the separation (in standard deviations) since the $\sqrt{\dot{S} \Delta t} \approx \sqrt{\dot{S}_H \Delta t} \approx \sqrt{\dot{S}_L \Delta t}$ for $\dot{S} \Delta t > 10000$ counts. As the number of detectors increases, the separation between $\dot{S} \Delta t$ and $\dot{S}_H \Delta t$ (or $\dot{S}_L \Delta t$) decreases and thus the minimum detectable off-specs pellet observed count rate \dot{B}_H (or \dot{B}_L) more closely approaches the good rate, \dot{S} .

As in the one-detector case, if the two equivalent worst measurements are considered, δ will decrease to the value δ_w . The value of δ_w is derived in the appendix for the two- and three-detector cases, but has not been computed for the tedious four- and five-detector cases. In Fig. 8, δ_w should be used in place of δ to determine the minimum detectable off-specs pellet with two measurements in the worst position. It is assumed (not proven) that any position between the best and worst will yield a minimum detectable off-specs pellet somewhere between that of the best position using δ and the worst position using δ_w .

3. Modified One-Point Models. In the case of two or more detectors, δ_w in Table I could be decreased by rejecting rods on adjacent points in different detectors; e. g., the k^{th} point from the

TABLE I

VALUES OF γ AND δ IN THE ONE-POINT MODEL (FIG. 8) REQUIRED TO KEEP THE GOOD AND BAD REJECTION RATES CONSTANT

n	γ	δ	$\gamma + \delta$	δ_w	$\gamma + \delta_w$
1	4.000	2.000	6.000	1.033	5.033
2	2.535	2.275	4.810	1.416	3.951
3	1.857	2.427	4.284	1.616	3.473
4	1.440	2.529	3.969	ND ^a	ND ^a
5	1.146	2.604	3.750	ND ^a	ND ^a

^aND = not determined

first detector and either the k-1, k, or k+1 point from the second detector would cause rejection. This model would not affect the results for a pellet in the best measuring position (because the pellet effectively influences only one point) but would allow more rejections for a pellet being measured near the worst position. Other ramifications of this model are briefly discussed in the appendix.

4. Multiple Detectors as One Detector. If two or more detectors (all identical) are located at the channel exit of PAPAS and the detectors are operated such that each views the same section of fuel for each TOC point, then the results for each TOC point can be summed to yield a single series of TOC points. Thus, the n multiple detectors act as a single detector with a count rate of $n\dot{S}$ (assuming no cross-talk between detectors and no loss of signal between detectors), and the models of Sec. IV. A. 1 can be used. This has the advantage over the multiple detector models in Sec. IV. A. 2 that the good rod rejection rate does not increase as the number of detectors increases.

B. Two-Point Models

A two-point model will be defined as requiring two adjacent points of the sequence of measured points to lie outside a specified tolerance interval of a known nominal mean value of TOC for a certain rod fissile loading. Clearly, this model is well suited for pellets being measured in the worst position since two equivalent measurements are provided. Conversely, this is not a reasonable model to use in the best measuring position because it is assumed that only one TOC point involving the bad pellet is available for the best position. As in the one-point models, a good and a bad point (indicating a minimum detectable off-specs pellet) rejection rate of 0.00634% and 97.73%, respectively, will be used.

1. One Detector. The one-detector version of the two-point model will reject a rod if any two adjacent points lie outside and on the same side of the tolerance interval. To keep the speci-

fied good and bad rod rejection criteria, the γ and δ in Table I for n=2 must be used. The resulting two-point one-detector model is shown in Fig. 9. Comparing Fig. 9 with Fig. 7 reveals that for the worst pellet measurement position the two-point, one-detector model is slightly superior to the one-point, one-detector model because the absolute difference between $\dot{S}\Delta t$ and $\dot{S}_H\Delta t$ (or $\dot{S}_L\Delta t$) is less (the value of γ decreased more than the value of δ increased).

2. Multiple Detectors. In the two-point, multiple detector model two adjacent points both outside on the same side of the tolerance interval must occur in each of the detector TOC points at the same place in the sequence. The γ and δ in Fig. 8 can be determined as in previous cases. The probability of rejecting a good point (0.0000634) is $(1 - A_\gamma)\left(\frac{1 - A\gamma}{2}\right)^{2n-1}$ for n detectors. Solving the expression for the A_γ between 0 and 1 enables γ to be found. Similarly, the probability of rejecting a bad rod with a measured TOC of $\dot{S}_H\Delta t$ (or $\dot{S}_L\Delta t$) is $\left(\frac{A_\delta + 1}{2}\right)^{2n}$ which is set equal to 0.9773. Finding A_δ allows δ to be determined. Table II shows the results for up to three detectors (δ_w is used instead of δ because only the worst measurement case applies in two-point models because a pellet in the best measuring position is assumed to be measured only once). Comparing the γ and δ_w in Tables I and II shows that analyzing the sequence of data points using a two-point model will increase

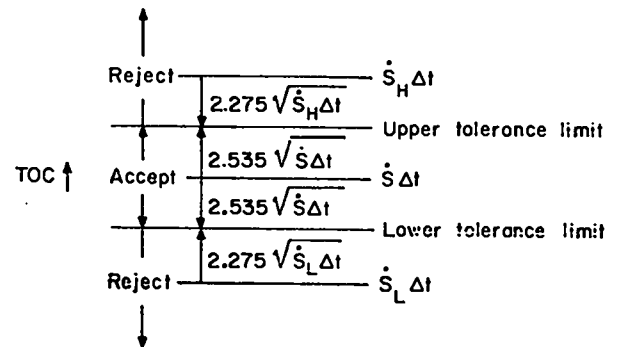


Fig. 9. Two-point, one-detector model which requires two adjacent TOC points to lie in the same reject region.

TABLE II
VALUES OF γ AND δ_w FOR THE TWO-POINT MODEL
TO KEEP THE GOOD AND BAD PELLET
REJECTION RATES CONSTANT

n	γ	δ_w	$\gamma + \delta_w$
1	2.535	2.275	4.810
2	1.440	2.529	3.969
3	0.924	2.665	3.589

the probability of detecting an off-specs pellet in the worst position for a system with a single detector; however, if the system has two or more detectors, a two-point model will not detect off-specs pellets as well as the one-point model because the model is too restrictive.

V. NUMERICAL RESULTS

Using the previously described models and definitions, several quantities may be examined by solving Eq. (8) numerically. The minimum detectable high or low off-specs pellet for a given system is found as follows:

- 1) \dot{S}_H is determined from the equation $\dot{S}\Delta t + \gamma\sqrt{\dot{S}\Delta t} = \dot{S}_H\Delta t - \delta\sqrt{\dot{S}_H\Delta t}$ using the methods of linear iteration³ where \dot{S} , Δt , γ , and δ are known quantities (see Fig. 8). \dot{S}_L is determined from the above expression with \dot{S}_L replacing \dot{S}_H , $-\gamma$ replacing γ , and δ replacing $-\delta$.
- 2) The minimum detectable pellet rate \dot{B}_H (or \dot{B}_L) is determined from Eq. (8) where $\text{TOC} = \dot{S}_H\Delta t$ (or $\dot{S}_L\Delta t$) and every quantity is known except \dot{B} . \dot{B} is determined from the regula falsi method³ and is defined to be \dot{B}_H (or \dot{B}_L), the minimum off-specs pellet which will be detected by 97.73% of all measurements.

PAPAS has the following characteristics:

- 1) the detector response function has a FWHM of 1.2 in., and
- 2) typical rod feed rates are 1.6 in./sec (8 ft/min) which yields an \dot{S} of ~ 90000

counts/sec for a 3% enriched PWR fuel rod using a 400 μg ^{252}Cf neutron source.

Typical pellet lengths are 0.6 in. for PWR and BWR fuel (newer nuclear reactor designs will have smaller pellet lengths). The numerical results presented in this section illustrate the effect of changes in some of the system parameters on the minimum detectable off-specs pellet rate \dot{B}_H (or \dot{B}_L). The relative deviation of the minimum detectable high and low off-specs pellet from \dot{S} are virtually identical, with the low pellet being slightly easier to detect. Relative deviations are examined rather than absolute deviations because the former is more useful in this application. In addition, one is able to get a feeling as to the effect of changes in other types of fuel rod scanning systems which have characteristics within the range examined here.

A. One-Point Models

1. One Detector. One quantity which must be optimized is the time interval Δt during which delayed gamma-ray counts are accumulated from the detector. An optimum Δt should exist because as Δt tends to zero, the relative statistics of a TOC point become quite poor, and as Δt tends to infinity, the bad pellet will only be in the detector window for a small fraction of the time interval Δt , which would make it difficult to detect. Figure 10 shows the minimum detectable off-specs pellet relative to the good counting rate \dot{S} as a function of Δt for several values of \dot{S} . Each pellet position has a different optimum Δt --independent of \dot{S} --to maximize the sensitivity of the measurement. The optimum times are 0.95 sec for the best pellet measuring position, 0.80 sec for the average, and 0.45 sec for the worst (each case to the nearest 0.05 sec increment). Notice that the distance of travel for a pellet in the best measuring position is $(0.95 \text{ sec}) \times (1.6 \text{ in./sec}) = 1.52 \text{ in.}$, which is about 1.25 times the detector FWHM. This represents the portion of the detector which has the largest response. It is important to note that for the worst measuring position, the optimum Δt is

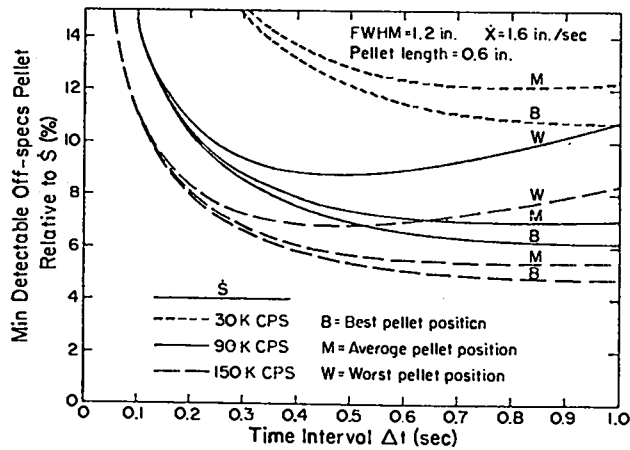


Fig. 10. Minimum detectable off-specs pellet as a function of the counting time Δt for various pellet measuring positions and three values of \dot{S} .

equal to one-half of the optimum Δt for the best measuring position; therefore, the expected value of the sum of the two worst measurement TOC points with its optimum Δt would equal that of the best TOC point for the optimum Δt of the best position. The optimum Δt for the middle position shows that the nonlinearity in the detector response results in a nonlinearity of optimum Δt as a function of position of the pellet during measurement.

In order to choose an optimum Δt for the system, independent of pellet measurement position, notice that the best and middle curves are reasonably flat over a large Δt increment in Fig. 10; thus an optimum Δt would appear to be in the 0.6- to 0.7-sec range because the worst, average, and best curves have not yet become much larger than their respective minimums. Figure 11 shows this in a different way: each of three pellet measuring positions (B, M, W) is shown for each of the three optimum times. It is clear that the minimum detectable off-specs pellet for the three positions is quite sensitive to the Δt chosen. A Δt of 0.6 sec will be chosen as optimum for the system since this Δt minimizes the product of the minimum detectable off-specs pellets for the best and the worst cases.

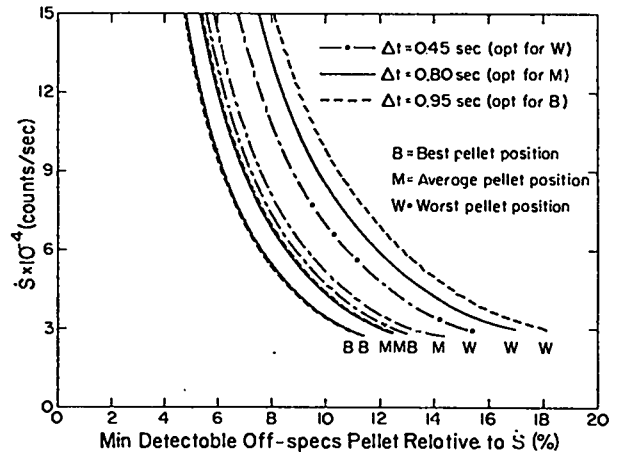


Fig. 11. \dot{S} vs the minimum detectable off-specs pellet for three pellet measuring positions and three values of the counting time Δt .

The above discussion, which was for 0.6-in.-long pellets, can be generalized to pellets of any length as shown in Fig. 12. The general trend, as one might expect, is that the optimum Δt for detecting a single pellet increases as the pellet length increases. For small pellet lengths, the optimum Δt approaches an asymptotic value because the FWHM of the detector is much greater than the length of the pellet. Again, the optimum Δt is independent of the effective good pellet emission rate \dot{S} , and the optimum Δt for the best position is twice that of the worst position.

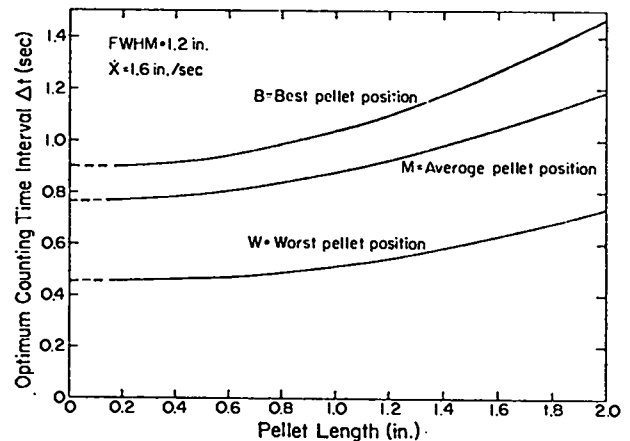


Fig. 12. Optimum counting time interval Δt as a function of the pellet length for three pellet measuring positions.

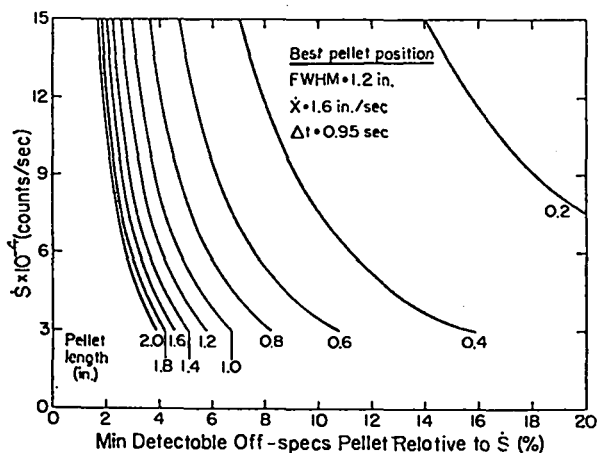


Fig. 13. \dot{S} vs the minimum detectable off-specs pellet for various pellet lengths in the best measuring position.

The effect of pellet length on the minimum detectable off-specs pellet for the best and worst measuring positions for a single measurement is shown in Figs. 13 and 14 for their respective optimum Δt s. These figures clearly show that the longer the pellet is, the smaller the deviation of the bad pellet from the good pellets to be detected for a specified \dot{S} . As an example, a 0.6-in.-long bad pellet in the best position surrounded by good pellets with an \dot{S} of 90000 counts/sec must deviate from \dot{S} by at least $\pm 6.2\%$ to be detected with this

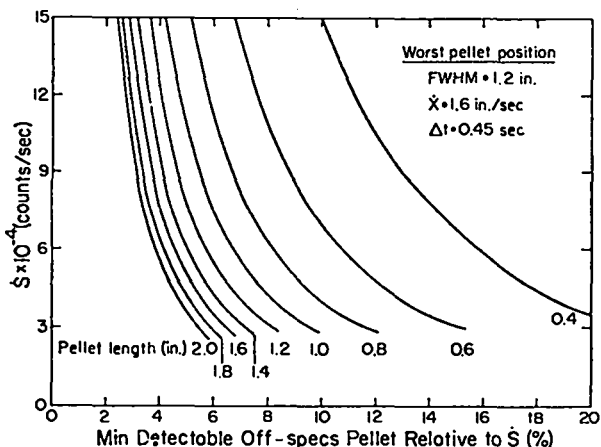


Fig. 14. \dot{S} vs the minimum detectable off-specs pellet for various pellet lengths for a single measurement in the worst position.

model; i. e., a 0.6-in.-long bad pellet in the best position with a \dot{B} of ≥ 95580 or ≤ 84420 counts/sec would be detected by $\geq 97.73\%$ of the measurements. The minimum detectable deviations of two or three consecutive 0.6-in.-long bad pellets in the best position would have \dot{B} s of $\pm 3.3\%$ and 2.4% , respectively, from an \dot{S} of 90000 counts/sec.

For one, two, or three consecutive bad pellets in the worst position, the minimum detectable deviations from an \dot{S} of 90000 counts/sec for one measurement using this model would be $\pm 8.8\%$, $\pm 4.7\%$, and $\pm 3.4\%$, respectively, as shown in Fig. 14. This effect saturates as the pellet length approaches about two FWHM of the detector.

It is important to note that to translate the percentage deviation from \dot{S} into percent mass or enrichment deviation, a curve similar to Fig. 5 must be used; i. e., any nonlinearities in the response as a function of mass or enrichment must be taken into account.

The effect of varying the fuel rod feed rate is shown in Fig. 15 for PAPAS measuring rods composed of 0.6-in.-long pellets. As expected, there is more sensitivity at slower feed rates for a given \dot{S} . (In an instrument like PAPAS, \dot{S} will change slowly as \dot{X} changes because the time for

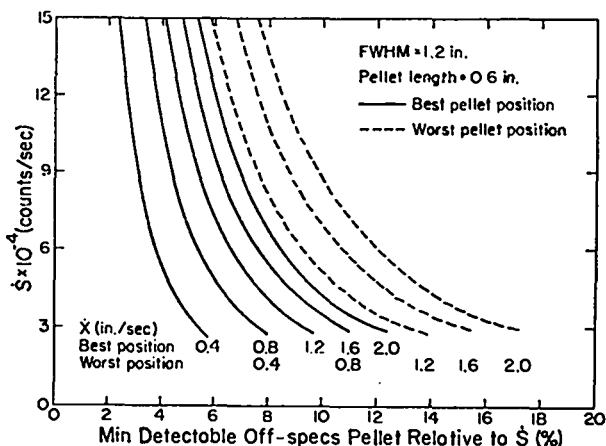


Fig. 15. \dot{S} vs the minimum detectable off-specs pellet for various rod feed rates \dot{X} with pellets in the best ($\Delta t = 0.95$ sec) and the worst (single measurement with $\Delta t = 0.45$ sec) measuring positions.

irradiation and resultant decay of the delayed gamma rays changes--this effect must be considered.) For example, the minimum detectable deviation for a bad pellet in the best measuring position moving at 2, 4, and 8 ft/min would be $\pm 3.1\%$, $\pm 4.4\%$, and $\pm 6.2\%$ of 90000 counts/sec; the minimum detectable percentage for the worst position would be $\pm 4.4\%$, $\pm 6.2\%$, and $\pm 8.8\%$, respectively. These results are for the optimum Δt of each case. Note the linear relationship between the good count rate \dot{S} and the fuel rod feed rate; e. g., the same relative percentage of \dot{S} is the minimum detectable bad pellet for $\dot{S} = 30000$ counts/sec, $\dot{X} = 0.4$ in./sec, and for $\dot{S} = 150000$ counts/sec, $\dot{X} = 2$ in./sec. There is also a two-to-one relationship between the best and worst positions at their respective optimum times because the ratio of the best to worst optimum Δt s is two.

Several questions concerning the detector FWHM are important; e. g., what effect does the FWHM have on sensitivity? Figure 16 shows that for a good pellet count rate of \dot{S} , the sensitivity decreases as the detector FWHM increases. The optimum Δt s were used for the best and worst measuring positions. In the actual case, a broader de-

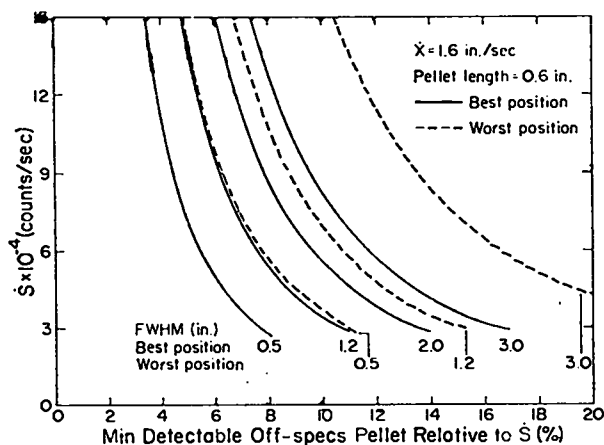


Fig. 16. \dot{S} vs the minimum detectable off-specs pellet for various FWHM of the detector response function for pellets in the best ($\Delta t = 0.95$ sec) and the worst (single measurement with $\Delta t = 0.45$ sec) measuring positions.

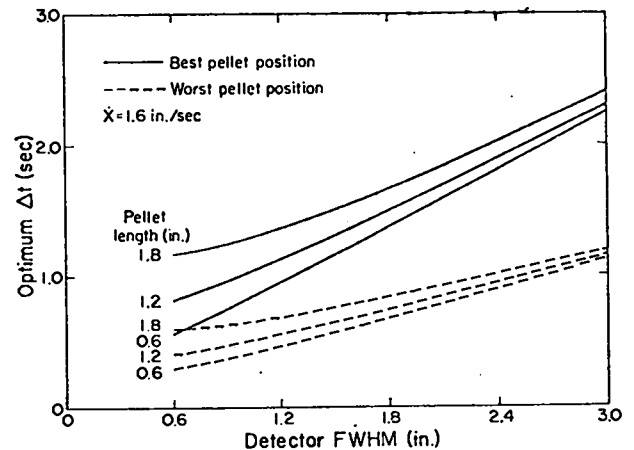


Fig. 17. Optimum counting time interval Δt vs the FWHM of the detector response function for various lengths of pellets in the best and worst measuring positions.

tector would also result in a larger count rate, and thus the question of what is the optimum size detector for a given pellet length must be considered for individual cases. This will not be attempted here. It is interesting to note, however, that the minimum detectable off-specs pellet is the same if the FWHM and \dot{S} are proportional. It is possible that doubling the detector thickness will cause the FWHM to increase by less than a factor of two because of the leakage into the sides of the crystal. In this case, a thicker crystal can be more sensitive if Poisson statistics are valid at the higher \dot{S} .

It is also of interest to examine the optimum times for the best and worst counting positions as a function of the detector FWHM for several pellet lengths. Figure 17 shows that the ratio of the best to worst optimum Δt s is two throughout the range of detector FWHM and pellet length. Thus, the absolute difference between best and worst optimum Δt s increases making the selection of an optimum system Δt more difficult.

A plot of the optimum Δt s for the best and worst measuring positions as a function of rod feed rate is shown in Fig. 18. As might be expected, the optimum Δt for a feed rate of \dot{X} is double the optimum Δt for a feed rate of $2\dot{X}$ because there is an optimum distance a pellet should travel in the detector to produce the minimum detectable off-specs pellet with this model.

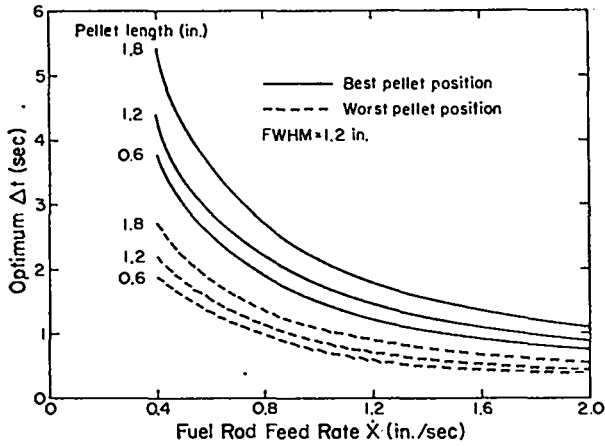


Fig. 18. Optimum counting time interval Δt vs the fuel rod feed rate \bar{X} for various lengths of pellets in the best and worst measuring positions.

2. Multiple Detectors. When more than one detector is used to scan a fuel rod and all detectors used are identical, the difference between $\dot{S}_H \Delta t$ and $\dot{S}_L \Delta t$ (or $\dot{S}_L \Delta t$) decreases as shown by Fig. 8 and Table I. In the case of one measure-

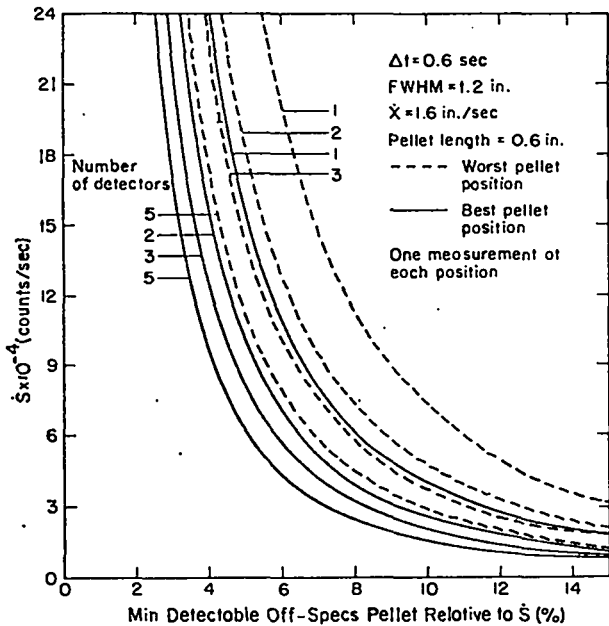


Fig. 19. \dot{S} vs the minimum detectable off-specs pellet for one or more identical detectors each viewing the pellet in the best or worst (single measurement) measurement position.

ment in either the best or worst position, Fig. 19 shows the increase in sensitivity for normal operating conditions for PAPAS, including $\Delta t = 0.6$ sec, as the number of measurements increases; e. g., the minimum detectable off-specs pellets in the best position ($\dot{S} = 90000$ counts/sec) for one, two, three, and five measurements are $\pm 6.6\%$, $\pm 5.3\%$, $\pm 4.7\%$, and $\pm 4.1\%$, respectively. The minimum detectable off-specs pellets for one measurement in the worst position are $\pm 9.0\%$, $\pm 7.2\%$, $\pm 6.4\%$, and $\pm 5.6\%$, respectively. By taking the second measurement in the worst position into account, the minimum detectable off-specs pellet in the worst position decreases to $\pm 7.5\%$, $\pm 5.9\%$, and $\pm 5.2\%$ for one, two, and three detectors as shown in Fig. 20. The cross-hatched bands in Fig. 20 are the range of the least off-specs pellet that can be detected by PAPAS with the one-point model for one, two, and three detectors. It is reasonable

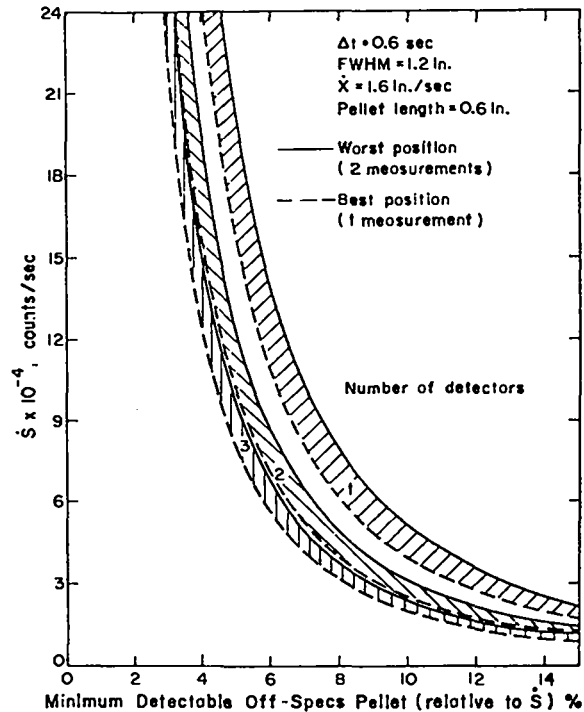


Fig. 20. \dot{S} vs the minimum detectable off-specs pellet for one or more identical detectors for a good rod rejection rate of 1.27% (200 TOC points per rod) and a bad point rejection rate of 97.73%.

to assume that any off-specs pellet not in the worst position when measured will be more easily detected with the one-point model than if it were in the worst position and received two identical measurements. The range of minimum detectable pellets for one, two, and three detectors is ± 6.6 to 7.5% , ± 5.3 to 5.9% , and ± 4.7 to 5.2% . Clearly, significant gains in sensitivity are made by adding detectors.

3. Multiple Detectors as One Detector.

Greater gains in sensitivity are made by summing each TOC point at a specified position on the rod from each detector. For example, for $\dot{S} = 90000$ counts/sec, two detectors summed to yield an equivalent $\dot{S} = 180000$ counts/sec, the minimum detectable off-specs pellet in the best position is 4.7% and in the worst position (two measurements) is 5.3% . This improvement over the range of 5.3% to 5.9% for two detectors in the previous section is because the good and bad rod rejection rates are not changed; i. e., only one TOC sequence is considered for the two detectors. Thus, summing the detector responses is preferred to treating the data separately for the models described.

B. Two-Point Models

Because of its limited applicability (i. e., only to pellets measured near the worst position), no calculations were performed; however, the minimum detectable pellet for the worst case for two identical measurements would be nearly the same for the one- and two-point models (compare the γ and δ_w columns in Tables I and II).

VI. CONCLUSIONS

Several models which should be relatively simple to implement on a scanning device have been examined. The models are based on "counting statistics" and represent the lower limit of the sensitivity of a scanning instrument. The TOC points could be analyzed with either the one- or two-point model or both. There is little to be gained, however, by using the two-point model

when a pellet in the best measuring position begins and ends the Δt interval outside of the detector (or nearly so) because the pellet is effectively measured only once. The minimum detectable off-specs pellet rates \dot{B} are listed in Table III as a function of good pellet rate \dot{S} and the number of detectors. The band of sensitivity is between the best and the worst (two identical measurements) measuring positions. Summing the TOC from multiple detectors at a given point increases the sensitivity of the instrument for the examples considered.

Even though the models are idealized, they do provide a basis to examine the sensitivity of a pellet-to-pellet system as a function of several system parameters. It is important to note that the good fuel will not be completely uniform because the fuel itself will vary over a certain range due to manufacturing processes. Consider Fig. 21. If $\dot{S}\Delta t$ represents the nominal value and the variation in the fuel is a small fraction of the tolerance interval $\dot{S}\Delta t \pm \gamma\sqrt{\dot{S}\Delta t}$, then the models as discussed are applicable; however, a larger fraction of good rods will be rejected because the normal distribution will not necessarily be symmetric with respect to the tolerance interval. The minimum detectable bad pellet will increase or decrease by some small amount, but, on the average, the results for the models will apply.

If the expected manufacturing variations in the good fuel content are a sizable fraction of the

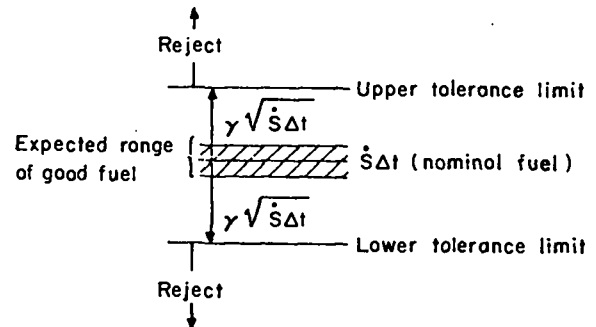


Fig. 21. General model for acceptance or rejection of a rod containing fuel with a variation which is small with respect to the tolerance interval.

TABLE III

MINIMUM DETECTABLE OFF-SPECS PELLETS RELATIVE
TO \dot{S} (%) USING THE ONE-POINT MODEL^a

Number of Detectors	Position of Pellet Measurement	\dot{S}					
		30K	60K	90K	120K	150K	180K
1	best	11.5	8.1	6.6	5.7	5.1	4.7
	worst (1 meas)	15.6	11.0	9.0	7.7	6.9	6.3
	worst (2 meas)	13.0	9.2	7.5	6.5	5.8	5.3
2	best	9.2	6.5	5.3	4.6	4.1	3.7
	worst (1 meas)	12.5	8.8	7.2	6.2	5.6	5.1
	worst (2 meas)	10.2	7.3	5.9	5.1	4.6	4.2
3	best	8.2	5.8	4.7	4.1	3.6	3.3
	worst (1 meas)	11.1	7.9	6.4	5.5	4.9	4.5
	worst (2 meas)	9.0	6.4	5.2	4.5	4.0	3.6
4	best	7.6	5.4	4.4	3.8	3.4	3.1
	worst (1 meas)	10.3	7.3	5.9	5.1	4.6	4.2
5	best	7.2	5.1	4.1	3.6	3.2	2.9
	worst (1 meas)	9.7	6.9	5.6	4.8	4.3	4.0

^a $\Delta t = 0.6$ sec, FWHM = 1.2 in., $\dot{X} = 1.6$ in./sec, pellet length = 0.6 in.; probability of point rejection because of minimum detectable pellet = 0.9773 and probability of good point rejection is 0.000634 for all cases.

$\dot{S}\Delta t \pm \gamma\sqrt{\dot{S}\Delta t}$ tolerance interval, then the one- and two-point models could be modified as shown in Fig. 22 where $\dot{Q}\Delta t$ and $\dot{P}\Delta t$ are the extremes of what is termed good fuel.

Without question, more sophisticated schemes can be used to analyze the data and to establish the number of bad pellets observed and how much out-of-specs these pellets are. It is hoped, however, that the models discussed here make the problem of scanning a fuel rod for an off-specs pellet easier to visualize and serve as a basis for further development of pellet-to-pellet analysis.

ACKNOWLEDGMENTS

The author wishes to thank H. O. Menlove and D. B. Smith of group A-1, J. R. Phillips of CMB-1, and R. H. Moore and R. J. Beckman of C-5 for enlightening discussions on various aspects of this subject.

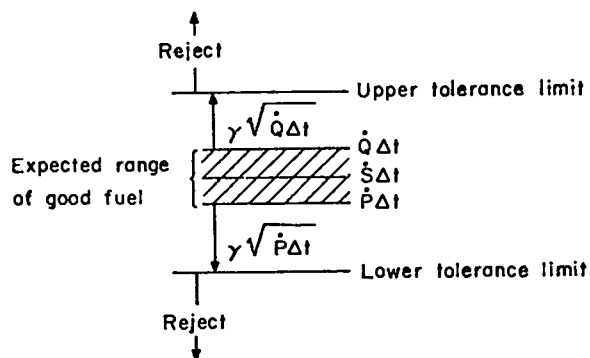


Fig. 22. General model for acceptance or rejection of a rod containing fuel with variations which are an appreciable fraction of the tolerance interval shown in Fig. 21.

REFERENCES

1. R. A. Forster, H. O. Menlove, J. L. Parker, and H. M. Forehand, Jr., "Performance of a Pellet-to-Pellet ²⁵²Cf Fuel Rod Assay System," *Trans. Am. Nucl. Soc.* **15**, 2, p. 680 (1972).
2. K. A. Brownlee, *Statistical Theory and Methodology in Science and Engineering* (John Wiley and Sons, Inc., 1967), 2nd Ed.
3. S. D. Conte, *Elementary Numerical Analysis* (McGraw-Hill Book Co., 1965).

APPENDIX
THE ONE-POINT MODEL FOR THE WORST MEASURING POSITION
FOR TWO AND THREE DETECTORS

Consider the case of a bad pellet being measured in the worst position (see Fig. 4). Two identical measurements of the bad pellet will then be made. There are two possibilities for each measurement: the point is either outside (O) the acceptance tolerance interval, or it is inside (I) the tolerance interval. Figure A-1 shows the possibilities for a high and low pellet. In each case, it is assumed that a TOC point with mean $\dot{S}_H \Delta t$ (or $\dot{S}_L \Delta t$) has such a small probability of being outside the tolerance interval on the low (high) side as to not be possible.

For the two equivalent measurements, there are a total of four possibilities for each detector: OI, IO, OO, II. For n detectors, there would be 4^n different combinations. The probability of a point being an O (lying outside the tolerance interval) is $A_\delta + (1 - A_\delta)/2 = (1 + A_\delta)/2$ where A_δ is the area of a normal distribution of mean μ between $\mu - \delta\sigma$ and $\mu + \delta\sigma$ (σ is the standard deviation of the distribution with mean μ). The probability of a point being an I (lying inside the tolerance interval) is $(1 - A_\delta)/2$. Thus, the probabilities for OI, IO, OO, and II, respectively, are $(1 + A_\delta)(1 - A_\delta)/4$, $(1 - A_\delta)(1 + A_\delta)/4$, $(1 + A_\delta)^2/4$, and $(1 - A_\delta)^2/4$. With these probabilities established, the probability of rejecting a rod using the one-point model for two and three detectors can be

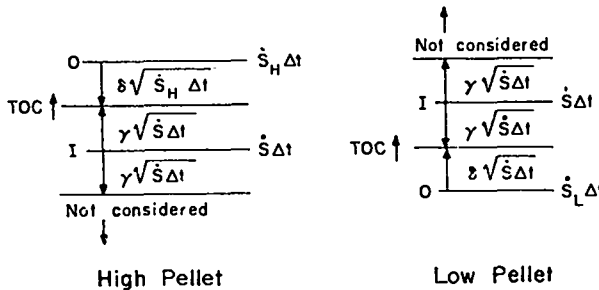


Fig. A-1. Models for a high and low pellet where O means outside the region of acceptance and I means inside the region of acceptance.

determined (the probability for one detector has been described in Fig. 7).

I. TWO DETECTORS

The sample space for two detectors is shown in Fig. A-2. The r , which signifies a rejection, occurs when two O points are at the same position in the TOC point sequence.

		Detector 1			
		OI	IO	OO	II
Detector 2	OI	r	Ⓐ	r	a
	IO	Ⓐ	r	r	a
	OO	r	r	r	a
	II	a	a	a	a

Fig. A-2. Sample space for two detectors with r being a rejection and a being an acceptance.

By summing the seven probabilities of rejection, the total probability of rejection $\text{Pr}\{r\}$ is

$$\text{Pr}\{r\} = \frac{1}{16} (7 + 12A_\delta + 2A_\delta^2 - 4A_\delta^3 - A_\delta^4). \quad (\text{A-1})$$

The total probability of accepting the rod as good for the two worst measurements, $\text{Pr}\{a\}$, is

$$\begin{aligned} \text{Pr}\{a\} &= \frac{1}{16} (9 - 12A_\delta - 2A_\delta^2 + 4A_\delta^3 + A_\delta^4) \\ &= 1 - \text{Pr}\{r\}. \end{aligned} \quad (\text{A-2})$$

Thus, when either $\text{Pr}\{r\}$ or $\text{Pr}\{a\}$ is known, A_δ can be found (there is only one real root between 0 and 1) along with the associated δ . For $\text{Pr}\{r\} = 0.9773$, $A_\delta = 0.84301$ and the associated $\delta_w = 1.416$, as listed in Table I.

If a modified one-point model were used (i. e., adjacent O's would also cause rejection), the circled a's in Fig. A-2 should be r's. Equa-

tions similar to Eqs. (A-1) and (A-2) can then be found and δ determined.

II. THREE DETECTORS

The sample space for three detectors contains 64 elements ($4^3=64$) and is shown in Fig. A-3. The r occurs when three O points are at the same position in the TOC point sequence.

The total probability of rejection $\Pr\{r\}$ (found by summing the fifteen r components) is

$$\Pr\{r\} = (15 + 42A_\delta + 33A_\delta^2 - 4A_\delta^3 - 15A_\delta^4 - 6A_\delta^5 - A_\delta^6)/64 \quad (A-3)$$

The probability of acceptance $\Pr\{a\}$ for the two points is

$$\Pr\{a\} = (49 - 42A_\delta - 33A_\delta^2 + 4A_\delta^3 + 15A_\delta^4 + 6A_\delta^5 + A_\delta^6)/64 \quad (A-4)$$

Again, the sum of $\Pr\{r\}$ and $\Pr\{a\}$ is unity. There is only one real root between 0 and 1. For $\Pr\{r\} = 0.9773$, $A_\delta = 0.89392$ and $\delta_w = 1.616$, as listed in Table I.

The circled a's in Fig. A-3 would become r's if a modified one-point model were used. Equations similar to Eqs. (A-3) and (A-4) can then be found and δ determined.

<p style="text-align: center;">DETECTOR 3:OI</p> <table border="0" style="margin-left: auto; margin-right: auto;"> <tr> <td colspan="2"></td> <th colspan="4" style="text-align: center;">Detector 1</th> </tr> <tr> <td colspan="2"></td> <th style="border-right: 1px solid black;">OI</th> <th>IO</th> <th>OO</th> <th>II</th> </tr> <tr> <th rowspan="4" style="vertical-align: middle;">Detector 2</th> <th style="border-right: 1px solid black;">OI</th> <td>r</td> <td style="text-align: center;">ⓐ</td> <td>r</td> <td>a</td> </tr> <tr> <th style="border-right: 1px solid black;">IO</th> <td style="text-align: center;">ⓐ</td> <td style="text-align: center;">ⓐ</td> <td style="text-align: center;">ⓐ</td> <td>a</td> </tr> <tr> <th style="border-right: 1px solid black;">OO</th> <td>r</td> <td style="text-align: center;">ⓐ</td> <td>r</td> <td>a</td> </tr> <tr> <th style="border-right: 1px solid black;">II</th> <td>a</td> <td>a</td> <td>a</td> <td>a</td> </tr> </table>			Detector 1						OI	IO	OO	II	Detector 2	OI	r	ⓐ	r	a	IO	ⓐ	ⓐ	ⓐ	a	OO	r	ⓐ	r	a	II	a	a	a	a	<p style="text-align: center;">DETECTOR 3:IO</p> <table border="0" style="margin-left: auto; margin-right: auto;"> <tr> <td colspan="2"></td> <th colspan="4" style="text-align: center;">Detector 1</th> </tr> <tr> <td colspan="2"></td> <th style="border-right: 1px solid black;">OI</th> <th>IO</th> <th>OO</th> <th>II</th> </tr> <tr> <th rowspan="4" style="vertical-align: middle;">Detector 2</th> <th style="border-right: 1px solid black;">OI</th> <td style="text-align: center;">ⓐ</td> <td style="text-align: center;">ⓐ</td> <td style="text-align: center;">ⓐ</td> <td>a</td> </tr> <tr> <th style="border-right: 1px solid black;">IO</th> <td style="text-align: center;">ⓐ</td> <td>r</td> <td>r</td> <td>a</td> </tr> <tr> <th style="border-right: 1px solid black;">OO</th> <td style="text-align: center;">ⓐ</td> <td>r</td> <td>r</td> <td>a</td> </tr> <tr> <th style="border-right: 1px solid black;">II</th> <td>a</td> <td>a</td> <td>a</td> <td>a</td> </tr> </table>			Detector 1						OI	IO	OO	II	Detector 2	OI	ⓐ	ⓐ	ⓐ	a	IO	ⓐ	r	r	a	OO	ⓐ	r	r	a	II	a	a	a	a
		Detector 1																																																																	
		OI	IO	OO	II																																																														
Detector 2	OI	r	ⓐ	r	a																																																														
	IO	ⓐ	ⓐ	ⓐ	a																																																														
	OO	r	ⓐ	r	a																																																														
	II	a	a	a	a																																																														
		Detector 1																																																																	
		OI	IO	OO	II																																																														
Detector 2	OI	ⓐ	ⓐ	ⓐ	a																																																														
	IO	ⓐ	r	r	a																																																														
	OO	ⓐ	r	r	a																																																														
	II	a	a	a	a																																																														
<p style="text-align: center;">DETECTOR 3:OO</p> <table border="0" style="margin-left: auto; margin-right: auto;"> <tr> <td colspan="2"></td> <th colspan="4" style="text-align: center;">Detector 1</th> </tr> <tr> <td colspan="2"></td> <th style="border-right: 1px solid black;">OI</th> <th>IO</th> <th>OO</th> <th>II</th> </tr> <tr> <th rowspan="4" style="vertical-align: middle;">Detector 2</th> <th style="border-right: 1px solid black;">OI</th> <td>r</td> <td style="text-align: center;">ⓐ</td> <td>r</td> <td>a</td> </tr> <tr> <th style="border-right: 1px solid black;">IO</th> <td style="text-align: center;">ⓐ</td> <td>r</td> <td>r</td> <td>a</td> </tr> <tr> <th style="border-right: 1px solid black;">OO</th> <td>r</td> <td>r</td> <td>r</td> <td>a</td> </tr> <tr> <th style="border-right: 1px solid black;">II</th> <td>a</td> <td>a</td> <td>a</td> <td>a</td> </tr> </table>			Detector 1						OI	IO	OO	II	Detector 2	OI	r	ⓐ	r	a	IO	ⓐ	r	r	a	OO	r	r	r	a	II	a	a	a	a	<p style="text-align: center;">DETECTOR 3:II</p> <table border="0" style="margin-left: auto; margin-right: auto;"> <tr> <td colspan="2"></td> <th colspan="4" style="text-align: center;">Detector 1</th> </tr> <tr> <td colspan="2"></td> <th style="border-right: 1px solid black;">OI</th> <th>IO</th> <th>OO</th> <th>II</th> </tr> <tr> <th rowspan="4" style="vertical-align: middle;">Detector 2</th> <th style="border-right: 1px solid black;">OI</th> <td>a</td> <td>a</td> <td>a</td> <td>a</td> </tr> <tr> <th style="border-right: 1px solid black;">IO</th> <td>a</td> <td>a</td> <td>a</td> <td>a</td> </tr> <tr> <th style="border-right: 1px solid black;">OO</th> <td>a</td> <td>a</td> <td>a</td> <td>a</td> </tr> <tr> <th style="border-right: 1px solid black;">II</th> <td>a</td> <td>a</td> <td>a</td> <td>a</td> </tr> </table>			Detector 1						OI	IO	OO	II	Detector 2	OI	a	a	a	a	IO	a	a	a	a	OO	a	a	a	a	II	a	a	a	a
		Detector 1																																																																	
		OI	IO	OO	II																																																														
Detector 2	OI	r	ⓐ	r	a																																																														
	IO	ⓐ	r	r	a																																																														
	OO	r	r	r	a																																																														
	II	a	a	a	a																																																														
		Detector 1																																																																	
		OI	IO	OO	II																																																														
Detector 2	OI	a	a	a	a																																																														
	IO	a	a	a	a																																																														
	OO	a	a	a	a																																																														
	II	a	a	a	a																																																														

Fig. A-3. Sample space for three detectors.